

JCTC

Journal of Chemical Theory and Computation

DFT Calculations on Charge-Transfer States of a Carotenoid-Porphyrin-C₆₀ Molecular Triad

Tunna Baruah[†] and Mark R. Pederson^{*,‡}

University of Texas at El Paso, El Paso, Texas 79968,

and Naval Research Laboratory, Washington, D.C. 20375

Received January 13, 2009

Abstract: We present a first-principles study on the ground and excited electronic states of a carotenoid-porphyrin-C₆₀ molecular triad. In addition, we illustrate a method for using DFT-based wave functions and densities to simulate complicated charge-transfer dynamics. Since fast and efficient calculations of charge-transfer excitations are required to understand these systems, we introduce a simple DFT-based method for calculating total energy differences between ground and excited states. To justify the procedure, we argue that some charge-transfer excitations are asymptotically ground-state properties of the separated systems. Further justification is provided from numerical experiments on separated alkali atoms. The donor-chromophore-acceptor system studied here can absorb and store light energy for several hundreds of nanoseconds. Our density-functional calculations show that the triad can possess a dipole moment of 171 D in a charge-separated state. The charge-transfer energy technique is used to obtain the energies of the excited states. The charge separated excited states with a large dipole moment will create large polarization of the solvent. We use a model to estimate the stabilization of the excited-state energies in the presence of polarization. The calculated excited-state energies are further used to calculate the Einstein's A and B coefficients for this molecular system. We use these transition rates in a kinetic Monte-Carlo simulation to examine the electronic excitations and possible charging of the molecule. Our calculations show that the solvent polarization plays a crucial role in reordering the excited-state energies and thereby in the charge-separation process.

Introduction

Solar energy is an abundant source of alternative energy. Nearly 75% of the solar radiation striking the upper atmosphere reaches the surface of the earth. The natural light harvesting systems such as plants or bacteria have evolved in ways that allow for a relatively efficient mechanism for converting and storing solar energy. This is done through a complex network of donor–acceptor systems which funnel the absorbed energy into a reaction center where the charge separation occurs. To replicate such light-harvesting systems, a plethora of donor–acceptor molecular diads and triads have

been synthesized and tested for efficient photovoltaic properties. In this paper, we study from first principles one such molecular donor–acceptor triad system containing a carotenoid, a porphyrin, and a C₆₀ molecule.

This carotenoid-porphyrin-C₆₀ molecular triad (see Figure 1) was first synthesized by Liddell et al.,¹ and many experimental studies have been reported (see refs 2–4 and references therein). In the experiments a pulse laser at 590 nm was used to excite the porphyrin which then leads to a cascade of transitions between the three components. The charge-separated state was found to have a lifetime of hundreds of nanoseconds. This charge-separated state has a large dipole moment of 153 D.² The large dipole moment and long lifetime can be exploited to build a molecular solar-cell.

* Corresponding author e-mail: pederson@dave.nrl.navy.mil.

[†] University of Texas at El Paso.

[‡] Naval Research Laboratory.

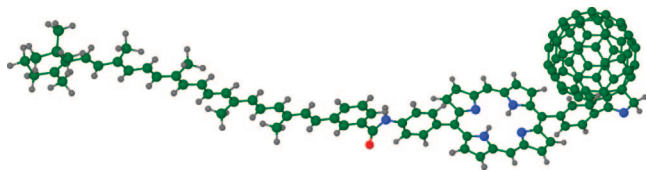


Figure 1. The triad molecule containing a carotenoid-porphyrin-buckyball.

It is known that photoinduced charge transfer (CT) as seen in photosynthesis is a complex nonradiative process where the transfer of energy depends on many different physical characteristics of the system. Developing a first-principles method that is both fast and relatively accurate presents a significant challenge as there are many different effects that must be included. Effects that must be included to get a full quantitative understanding of photoinduced charge transfer include vibrational effects, electronic transitions, energy transport, and polarization effects. In this work we discuss some computationally efficient density-functional strategies that can be used and refined to allow for some predictive understanding in this area. We combine various methods to obtain a reliable description of the transitions involving absorption of light. Here we present a simple density-functional theory (DFT) based approach for the study of excited charge-separated states, the solvent polarization and stabilization of the charge separated states, and finally any possible radiative transitions. From a combination of density-functional-determined properties a kinetic Monte-Carlo method is used to determine charge-transfer rates. We show that the radiative transitions leading to charge separation are rare events but can be accelerated through a bias caused by an external electric field or due to the presence of counterions. This study is done for radiation density of solar radiation and forms a sequel to our earlier study of the electronic ground-state properties of this molecular triad.⁵

Simple Charge Transfer Systems

One of the goals of this paper is to perform simulations on large molecules for which charge-transfer energies and rates are the relevant figures of merit. It is highly desirable to find fast methods for calculating such excitation energies. Davidson and Nitzsche⁶ performed delta-SCF calculations on excited-state within Hartree–Fock early on. They identified at least one case where errors could be made if orthogonality between the ground and excited-state singlets were not maintained. From the standpoint of excited-state calculations within density-functional-based approximations, Perdew and Levy discussed conditions for which extrema of the density-functional energy could be used for excited states in a seminal paper.⁷ It is interesting to note that in introducing their ideas they include a quotation from an even earlier piece of literature that is worthwhile reflecting on here: “One of the most important and controversial questions in density-functional theory concerns the extent to which excited states can be studied by these methods”.⁸ While the statement on the controversy is probably as true today as it was in 1984–1985, the need for considering many ways to address this problem is probably more urgent since we are at least a

quarter of a century closer to the time when replacements and/or more efficient uses of petroleum resources will be required. The ability to calculate excited states will be key to availing *this generation* of new scientists with tools for computationally improving many technologies that are needed for addressing relatively short-term societal needs. While the scientific debate and iterative improvement of the most ideal way for computing excited states should continue, progress toward deploying a multifaceted array of computational methods for addressing excited states during the next quarter of the century could prove to be truly convenient with respect to more effectively developing technologies that address current issues.

As such we introduce an efficient albeit imperfect means for the calculation of charge-transfer energies in a forthcoming section. The method could be used with almost any type of functional or mean-field quantum-mechanical theory and could be improved upon. For practical reasons it is most attractive to determine the effectiveness of such a method on the standard density-functional methods. In particular we note that we have not relied on either self-interaction corrections^{9–11} or exact exchange to stabilize the process. Instead, we include the strong constraint of orthogonalization to the many-electron ground-state reference state. Before discussing this in reference to the light-harvesting triad, we perform some calculations on very simple charge-transfer systems.

Charge Transfer within Ground-State DFT. In this section, we carefully discuss the charge-transfer energy that relates to removal of an electron from one neutral alkali atom and subsequent attachment of this electron to a different albeit identical alkali atom that is at a large distance from the original atom. The purpose of this discussion is to show that this charge-transfer excitation energy depends entirely on ground-state properties of the alkali neutral and charged states. From the arguments presented here we conclude that even within the strictest possible formulation of density-functional theory, the lowest charge-transfer excitation energy in these systems is a ground-state property and is rigorously amenable to calculation within the strictest possible density-functional framework.

We start by considering the case of an isolated alkali atom with either a net positive or net negative charge. These systems are spin unpolarized, and therefore their ground-state energies and densities are rigorously attainable within the original and strictest version of density-functional theory. If we now turn on a static electric or magnetic field, the energy of the charged alkali atom changes due to two effects. To first order, there is direct interaction between the net charge of the alkali atom and the electric field. The system has no net moment so there is not a first-order interaction between a charged alkali and an applied magnetic field. In addition there are small second-order effects related to the field-induced polarization terms. The conclusion of this discussion is that the ground-state energy of a positively (U_I) or negatively (U_A) charged alkali atom is rigorously attainable from density-functional theory. From the definition of ionization energies and electron affinities, the energy of the charged ground states relative to the neutral ground states

Table 1. Calculated Ionization Energies (Ip) and Electron Affinities (A) of Hydrogen-Like Atoms^a

| atom | affinity | | ionization | | charge transfer | |
|------|----------|------|------------|------|-----------------|-------|
| | DFT | EXP | DFT | EXP | DFT | EXP |
| H | 0.76 | 0.75 | 13.6 | 13.6 | 12.84 | 12.85 |
| Li | 0.51 | 0.61 | 5.59 | 5.39 | 5.08 | 4.78 |
| Na | 0.55 | 0.55 | 5.36 | 5.13 | 4.81 | 4.58 |
| K | 0.51 | 0.50 | 4.45 | 4.34 | 3.93 | 3.84 |
| Rb | 0.51 | 0.49 | 4.22 | 4.17 | 3.71 | 3.62 |
| Cs | 0.48 | 0.47 | 3.83 | 3.89 | 3.35 | 3.42 |

^a Included in the table are results from large-basis sets PBE-GGA calculations and experiment.¹⁸ All energies are in eV.

are given by $U_I = U_o + I$ and $U_A = U_o - A$ with U_o being the energy of the neutral ground state. In many systems (including alkali atoms) I and A are both positive quantities according to the common sign conventions that we also use in this paper.

We now discuss the ground state of the neutral alkali atom. While the practice of using spin-polarized energy functionals is exceedingly well accepted and common in many applications, the original version of density-functional theory was only applicable to nondegenerate ground states. Early arguments to extending density-functional theory to spin-polarized ground states noted that an infinitesimal magnetic field would split the energy of a doublet state yielding a nondegenerate ground state. For the present case of interest (one unpaired electron outside of a closed shell), this simply means that we can in principle calculate the ground-state energy $U_o(B)$ as a function of applied field and extract the ground-state energy at zero field and the spin susceptibility. From this discussion it follows immediately that for two infinitely separated alkali atoms, the charge-transfer energy is a ground-state property given by $C = I - A$. Further, for two well-separated alkali atoms the charge-transfer energy is given by $I - A - 1/R$ with R being the separation between the two atoms. The $1/R$ stabilization is simply due to the classical coulomb interaction of two charged particles and also immediately falls out by considering the difference of the coulomb energy of two neutral atoms compared to two oppositely charged atoms.

This energy is correct to $O(R^{-4})$ for the case of two alkalis. The lowest correction term arises from the polarization-induced stabilization of each ion that occurs due to the electric field of the other counterion. This energy depends linearly upon the sum of the polarizabilities of the counterions. As in the case of the coulomb interaction, monopole-induced-dipole stabilization as well as other electrostatic interactions between the separated ion are extractable from ground-state density-functional calculations. In Table 1, the charge-transfer energies for pairs of alkali atoms are presented and compared to experiment using the PBE-GGA.¹² As discussed below, the agreement with experiment is good.

Charge-Transfer Energies between Two Well-Separated Alkalis. In Table 1, we present electron affinities calculated within the PBE-GGA for H, Li, Na, K, Rb, and Cs. Very extensive basis sets were used for these calculations. We started with the basis sets developed by Porezag and Pederson¹³ for ground-state density-functional calculations. The NRLMOL code was used for the calculations.^{14–17} This

work optimizes each Gaussian exponent in the problem by variationally minimizing the atomic energy with respect to variation of each nonlinear exponent and the linear expansion coefficients. As discussed in that paper the shortest range Gaussian function must scale as $Z^{10/3}$ to ensure that the energy of the 1s-core electrons are all converged to the same absolute error. Since the anions are expected to be more diffuse than the neutral atoms, we have appended additional long-range single-Gaussian functions to the basis as well and have also used some r^2 gaussians to represent the s-functions. For lithium we have used a total of 11 Gaussian exponents that range between 3200 and 0.005 bohr⁻². In addition to 11 s- functions generated from these maximum and minimum values we have also included the r^2 s-type gaussians that fall in the range of 1.28 to 0.02827 bohr⁻². For Rb, which has a much larger Z , we have used a total of 23 bare gaussians ranging between 84105050 and 0.005 bohr⁻². The basis for the functions contained all 23 of the single Gaussian and also included 17 r^2 functions with decay parameters ranging between 9612 and 0.0211 bohr⁻². The p-type orbitals utilized 20 functions ranging between 81517 and 0.005 bohr⁻². The 17 d-type functions with the same decay constants as the r^2 s-type functions were used. The calculations in Table 1 are well converged with respect to basis set. Examination of the tables reveals that from calculations on the isolated species, the charge-transfer energies of these systems can be calculated with very high accuracy as compared to experiment.¹⁸

If one attempts to self-consistently determine the energy of the well separated cation and anion using a standard ground-state density-functional the system quickly finds the real ground state consisting of two neutral atoms. Part of the problem is that the standard DFT iterative method reorders occupation numbers to account for Fermi-level misalignments. This sort of a problem is related but slightly different than the problem that occurs when two well separated systems with different electronegativities are computationally treated as a single system. In such cases, fractional charges are known to occur on the atoms.^{19–21}

The misalignment present for the cation–anion pair is in fact physical in this case as it correctly identifies the fact that the electronic configuration of the charge separated state is not the ground state. A computational method that allows for minimization of the functional within the constraint of orthogonality to the ground state does not have this shortcoming. In the forthcoming sections where we wish to apply this procedure to excitations with well-separated but not infinitely separated electron–hole pairs, we introduce a constrained variational method to perform the calculations.

It has long been recognized that the commonly used density-functionals are not self-interaction free.^{9–11} As touched upon elsewhere in this paper and a multitude of other papers (see ref 22 and references therein), one of the manifestations of functionals devoid of self-interaction corrections are unbound anions. By unbound, one generally means that the orbital eigenvalue lies above zero. However highly charged anionic systems are experimentally known to exist for long periods of time. At the macroscale, such systems are referred to as capacitors, but nanoscale analogs

such as molecular dianions are known to exist. Compton et al. have provided convincing arguments as to why a dianion can be long-lived even if the dianion is unstable relative to the anion. See refs 23 and 24 and references therein. To the extent that such systems are experimentally known to be unstable the best-possible quantum-mechanical theory, which would be self-interaction free, should provide positive eigenvalues and unbound states. There should be a sensible way of describing such systems within a quantum-mechanical framework. In this regard, the shortcoming of unbound anionic systems within standard DFT functionals is only one example of a larger class of problems, some of which are experimentally observable, that should have a sensible solution. Convergence in such systems, if this word can be used, would most likely be obtained through the use of either implicit or explicit constraints. By implicit constraints we refer to the use of localized basis functions or possibly imposition of a vanishing boundary condition. By explicit constraints we refer to methods that would be similar in scope to those suggested by Watson²⁵ and Boyer²⁶ for stabilizing anions and dianions or more recently by Van Voorhis for stabilizing charge-transfer states.^{27–29} In each of these cases, a methodology has been developed for including external potentials that force a charge state or charge rearrangement that would be otherwise unstable. The tacit assumption in all of these cases is that the resulting structure is representative of physical systems that could be prepared through the application of external electric fields. Imposition of constraints has proven to be valuable for a variety of practical applications.

A Constrained Excited-State Method

In this section we discuss an attempt for developing a practical means for calculating excited states using the standard approximations to the density-functional theory. Prior to the development of density-functional theory, a transition-state approach due to Slater which used the X_α -method as an approximation to Hartree–Fock was investigated and used with some success for describing localized excitations in atoms and defects. From the standpoint of using density-functional-based approximations, Perdew and Levy discussed conditions for which extrema of the density-functional theory could be used for excited states.⁷ Further they review efforts aimed at extending DFT to the lowest-energy state of each symmetry and the efforts due to Theophilou³⁰ which asserts that the M lowest-energy states are a functional of the average density of these states provided that the M lowest-energy states are constrained to be orthogonal to one another. In regard to such attempts they note that not all excited-state densities are expected to be v -representable.

In the method proposed below, a variational formalism for excited states is developed; however, the variations are performed in a way that do not require v -representable excited-state densities. In developing this method we introduce a constraint of orthogonality between the many-electron Slater determinants that are constructed from the ground- and excited-state of interest. Imposition of such a constraint would appear naturally if one thinks in terms of many-

electron wave functions. This constraint leads to a set of single-particle orbitals that do not move in a local Hamiltonian and therefore do not guarantee that the resulting excited-state density is v -representable.

To motivate this method, we assume that a set of orthonormal single-particle orbitals have been determined from a mean-field method such as Hartree–Fock or density-functional theory. Starting with the expression for the total energy and the set of single-particle orbitals that minimize the energy we then wish to build a set of approximate many-electron excited-state Slater determinants that are efficiently optimized from the standpoint of a variational principle. The variational principle that seems most reasonable is to require that the energy of an approximate excited state is minimized relative to all possible variations that maintain orthogonality of the excited state to the ground-state wave function. Once such a set of wave functions are identified, it is possible to imagine using the ground and low-lying excited configurations as a basis for constructing a more exact set of ground- and excited-state orbitals through a configuration-interaction procedure. Further it is assumed that the energies of the resulting set of Slater determinants can be reasonably well approximated from the energy functional that has been used to construct the ground-state energy. In this work, we limit our applications to standard GGA energy functionals. However, the formalism described here can be used within any of the functionals developed by Perdew and collaborators. The computational formalism described here is motivated with the idea that the precise functional that would lead to the best excited states could be developed in concert with the use of this variational procedure. In order to prevent the procedure from leading to a set of orbitals that have collapsed into the ground-state manifold, we introduce the constraint that the many-electron excited-state Slater determinants must be orthogonal to the many-electron ground-state Slater determinant that is composed of the ground-state orbitals. Before continuing we emphasize that if we construct two many-electron Slater determinants (Φ) and (Ψ) from two different sets of orthonormal wave functions ($\phi_1, \phi_2, \dots, \phi_N$) and ($\psi_1, \psi_2, \dots, \psi_N$), the overlap of the two many-electron wave functions ($\Phi|\Psi$) vanishes as long if $(\phi_i|\psi_j) = 0$ for some value of i and all values of j . Alternatively the overlap of the two many-electron wave functions vanishes if $(\psi_i|\phi_j) = 0$ for some value of i and all values of j .

We begin by constructing a single Slater determinant from the single particle self-consistent lowest N Kohn–Sham orbitals ϕ to describe the ground-state wave function as

$$\Psi(\{\vec{R}_n\}) = A(\phi_1\phi_2\cdots\phi_N) \quad (1)$$

where N is the number of particles. Here, “ A ” represents the antisymmetrizing operator which simply makes an N -electron Slater determinant out of the N single-particle orbitals. The wave functions for single excitations can be constructed from $N - 1$ of the original occupied orbitals ϕ_i (with $i \neq h$) and an unoccupied orbital which we refer to as ϕ_p

$$\Phi = A(\phi_1\phi_2\cdots\phi_{h-1}, \phi_p, \phi_{h+1}\cdots\phi_N) \quad (2)$$

where subscripts h and p refer to the hole and particle states. It is important to emphasize the occupied ϕ -orbitals are only

defined up to an arbitrary unitary transformation so the most optimal hole state is only constrained to lie in the space spanned by the occupied Kohn–Sham orbitals. The ground-state density ρ_g is determined by the Kohn–Sham orbitals with occupancy f as $\rho_g = \sum_i f_i |\phi_i|^2$. The nonself-consistent density is then given by $\rho_{ex} = \rho_g - \rho_h + \rho_p$ where $\rho_h = |\phi_h|^2$ and $\rho_p = |\phi_p|^2$. The self-consistent ground-state Hamiltonian is

$$H_g = H(\rho_g) \quad (3)$$

Generally, one can approximate the excited-state Hamiltonian in terms of

$$H_{ex} = H(\rho_{ex})$$

However, it is generally not possible to self-consistently determine H_{ex} if one attempts to iterate using standard iterative procedures. Doing so will often lead to the collapse of the second set of orbitals onto the first set. It is clear that such a collapse violates the original orthogonality constraint between the excited-state and ground-state determinants.

To make further progress we first consider a parameter dependent perturbative Hamiltonian of the form

$$\Delta H = \alpha(H_{ex} - H_g) \quad (4)$$

where α is only a tuning parameter. The ϕ_h and ϕ_p are the active orbitals which start out orthogonal to one another and to all the passive ground-state Kohn–Sham orbitals. If we vary the passive excited-state orbitals in the space that is orthogonal to ϕ_h and ϕ_p , we are guaranteed to produce a total energy that is lower than that of the rigid excitation. Further the SD composed of these new passive orbitals and the particle orbital would still be orthogonal to the ground-state SD. To determine the improved excited-state passive orbitals we perturbatively update these orbitals using the following expression

$$\phi'_h = \phi_h + \alpha \sum_{j > N} \frac{\langle \phi_j | \Delta H | \phi_h \rangle \langle \phi_j |}{\epsilon_j - \epsilon_h} \quad (5)$$

and

$$\phi'_k = \phi_k + \alpha \sum_{j > N} \frac{\langle \phi_j | \Delta H | \phi_k \rangle \langle \phi_j |}{\epsilon_j - \epsilon_k} \quad k \neq h \quad (6)$$

In the above $h \leq N$ and $k \leq N$. Further, instead of holding the active particle orbital rigid, which would indeed be a somewhat unphysical constraint on the orbitals, it is possible to refine the method further by relaxing the particle orbital in the space of the unoccupied orbitals using exactly the same perturbative approach

$$|\phi'_p\rangle = |\phi_p\rangle + \alpha \sum_{j > N} \frac{\langle \phi_j | H' | \phi_p \rangle \langle \phi_j |}{\epsilon_j - \epsilon_p} \quad (7)$$

This approach is intuitively more palatable since it is unreasonable to expect the particle orbital to be an eigenfunction of the ground-state Hamiltonian. The resulting set of orbitals depart from orthonormality at second-order. To produce a set of α -dependent orthonormal orbitals we first

renormalize the relaxed hole orbital (giving us ϕ''_h). We then Schmidt orthogonalize all passive relaxed orbitals ϕ'_k ($k \neq h$) to the relaxed hole–electron ϕ''_h . Finally the passive occupied states and active particle states are orthonormalized using Löwdin’s method of symmetric orthonormalization.³¹ By following this prescription we are now furnished with a set of α -dependent orthonormal orbitals that can be used to construct an α -dependent Slater determinant that is orthogonal to the ground-state Slater determinant. The excited states can then be expressed as

$$\Phi_{ex} = A(\phi''_1 \phi''_2 \dots \phi''_{h-1} \phi''_{h+1} \dots \phi''_N; \phi''_p) \quad (8)$$

The orthogonality between the ground-state Slater determinant and the individual excited-state determinant follows since $\langle \phi'_i | \phi''_h \rangle = 0$ for $i \neq h$. The orthogonality to the ground state is achieved because it is possible to find a unitary transformation (actually there are an infinite number of such unitary transformations) on the original orbital set (ϕ_i) which creates a new set of orthonormal orbitals which span the same space as the Kohn–Sham ground-state orbitals and lead to the same density and energy. These orbitals can be written as $(\psi_1, \psi_2, \dots, \psi_{h-1}, \phi''_h, \psi_{h+1}, \dots, \psi_N)$ with ϕ''_h identically equal to the relaxed hole electron.

The density is then calculated from the occupied passive and active orbitals as

$$\rho' = \sum_j |\phi''_{j \neq h}|^2 + |\phi''_p|^2$$

From this density the coulomb energy and exchange correlation energies may be calculated, and the orbitals can also be used to calculate the kinetic energy and the interaction of the density with an external potential. The same procedure is repeated with different values of α . From a set of α and corresponding total energies, the α for lowest energy is determined. The best-excited-state Slater determinant can then be determined by minimizing the energy as a function of α . Once the best α is determined, this provides us with a new way of estimating an excited-state single-electron Hamiltonian H_{ex} which gives a new ΔH . Given the improved ΔH we can return to eq 4 above and further improve the estimation of the single-particle orbitals. The process can be iterated until self-consistency is established.

In this method the excited-state density is varied by varying the parameter α . In practice, three different α are chosen, and the α_{lowest} is varied using the Newton–Raphson method. The same procedure can again be repeated to refine the α_{lowest} parameter and thereby the energy. This method is inexpensive, since the diagonalization is not required and the α_{lowest} can be extracted relatively inexpensively. The only computationally intensive part is the calculation of coulomb energy for the new density ρ' . However, the procedure needs to be repeated for each set of the particle-hole excited states in question. Also the orthogonality between two excited states is not achieved exactly at present. However, this is a problem that can be solved as well using projection methods and/or

explicit orthonormalization methods similar to the ones discussed above.

Computational Details

The calculations reported here were carried out with the NRLMOL code.^{14–17} The calculations were performed at the all-electron level with generalized gradient approximation for exchange-correlation potential. The code uses a large Gaussian basis with polarization functions. The basis set for each atom uses the same set of primitive Gaussians thereby reducing computation. The coefficients of the contracted Gaussians are optimized for each atom.¹³ The grid for calculation is variational in that the error in integrals is minimized with respect to the number of points.¹⁵ Moreover, the coulomb potential is calculated analytically. For the triad calculations the electronic structures were calculated using 5 s-type, 4 p-type, and 2 d-type basis functions for carbon, nitrogen, and oxygen atoms. These were contracted from 12 primitive Gaussians for carbon and 13 primitives for oxygen and nitrogen atoms. For hydrogen 4 s-type and 3 p-type functions contracted from a set of 6 primitives were used. The calculations are done at the all-electron level and use generalized gradient approximation for exchange-correlation functionals.¹²

Results and Discussion

We have performed calculations for different systems from small atoms to large molecules. The purpose of this calculation is to examine the cases where the Δ SCF method will be more suitable and where the present method will have an edge. As the simplest case, we have calculated the excitation energies of the first and second row atoms H - Ar. Since our treatment is based on the perturbation method, the small atoms are expected to show the worst agreement with experiment. One way of improving the results for small atoms will be to include higher order terms in the expansion of the wave functions. Another point worth noting in closed shell inert atoms is the necessity for including the long-range Gaussians in the basis. In the inert atoms such as He, the excited electronic state will be spread over a much larger space than the tightly bound ground state which requires long-range Gaussians.

Applications to Atoms and Molecules. The results of our calculations on atoms along with the experimental values are tabulated in Table 2. The experimental values are taken from the NIST Atomic Structure Database. The values show that the perturbative treatment adopted in the present method does not perform very well for closed shell atomic systems. However, such a deficiency is expected due to the relatively large perturbation for the atoms.

We have performed calculations on several small atoms and molecules to gauge the applicability of the method. The HOMO–LUMO excitation energies for the singlet and triplet states are shown in Table 3 and are compared with other available values from the literature.^{32–37} All these calculations are spin unrestricted. The basis set effect is large in small molecules also. The basis set used here is large, but improvements can be made. The results are not perfect but

Table 2. Calculated Excited State Energies (eV) For Atoms Using the Constrained Orthogonality Method (COM), Δ SCF, and Experiment^a

| atom | state | COM | Δ SCF | expt |
|------|---|-------|--------------|-------|
| H | 2s | 11.95 | 9.90 | 10.20 |
| H | 2p | 10.78 | 9.91 | 10.20 |
| H | 3s | 12.44 | 11.69 | 12.09 |
| He | 1s2s(¹ S) | 22.32 | 20.32 | 19.82 |
| He | 1s2s(³ S) | 22.17 | 19.48 | 20.62 |
| He | 1s2p(¹ P) | 23.80 | 20.82 | 20.96 |
| He | 1s2p(³ P) | 23.67 | 20.38 | 21.22 |
| Li | 1s ² 2p | 1.89 | 1.89 | 1.85 |
| Be | 1s ² 2s2p(³ P) | 3.44 | 1.63 | 2.72 |
| Ne | [He]2s ² 2p ⁵ 3s(¹ S) | 17.91 | 16.74 | 16.62 |
| Na | [Ne]3p | 1.91 | 1.91 | 2.10 |
| Mg | [Ne]3s3p | 3.71 | 2.73 | 2.71 |
| Ar | 3s ² 3p5(2P(1/2)4s | 11.67 | 11.64 | 11.72 |
| Ar | 3s ² 3p5(2P(1/2)4p | 12.87 | 12.59 | 13.28 |
| Kr | 4s ² 4p ⁵ 5s | 10.23 | 10.17 | 9.91 |

^a See ref 11.

Table 3. Calculated Excited State Energies (eV) for Small Molecules Using the Constrained Orthogonality Method (COM), Δ SCF, and Experiment^{32–36a}

| system | state | COM | Δ SCF | expt |
|------------------|---------|-------|--------------|------|
| N ₂ | singlet | 8.49 | 8.48 | 9.31 |
| | triplet | 7.50 | 7.49 | 8.04 |
| H ₂ O | singlet | 7.50 | 7.45 | 7.40 |
| | triplet | 7.13 | 7.07 | 7.20 |
| CO | singlet | 7.20 | 7.51 | 8.51 |
| | triplet | 5.67 | 5.91 | 6.32 |
| CO ₂ | singlet | 9.04 | 8.70 | |
| | triplet | 8.02 | 8.13 | |
| O ₃ | singlet | 1.94 | 1.88 | 1.95 |
| | triplet | 1.43 | 1.36 | 1.45 |
| LiH | triplet | 3.15 | 3.07 | 3.25 |
| | singlet | 3.85 | 3.44 | 3.61 |
| HF | singlet | 11.41 | 11.65 | |
| | triplet | 11.38 | 8.61 | |
| HCN | singlet | 8.91 | 9.11 | |
| | triplet | 7.93 | 6.61 | |
| O ₂ | singlet | 1.65 | | 1.64 |

^a The theoretically calculated results are vertical excitations. For LiH, in the experimental column, we have used configuration interaction results of ref 37.

show reasonable accuracy. For small atoms and molecules, the relaxations of the passive orbitals due to a charge rearrangement is expected to be larger than relaxations due to less localized excitations in large molecules. In almost all cases, the constrained orthogonality method overestimates experiment. This could indicate that further iterations over the perturbative approach could improve the agreement between theory and experiment. Another point is that these are vertical excitations and therefore exclude the effects due to the rearrangements of ions.

Ground-State Properties of the Triad

We have optimized two different geometries of the triad molecule using density-functional theory at the all-electron generalized gradient level, details of which can be found in ref 5. A linear structure nearly 50 Å long was found to be lower in energy, and therefore all subsequent calculations are done on this structure. The ground state of the molecule has a permanent dipole moment of 9 Debye, and its highest

Table 4. Eigenvalues (eV) and Molecular Parentage of the Ten Highest Occupied and Ten Lowest Unoccupied Orbitals ($-\epsilon_{\text{Fermi}} = 4.30$ eV)

| hole | | | particle | | |
|-------|-------------|-----------------|----------|-------------|-----------------|
| index | $-\epsilon$ | parentage | index | $-\epsilon$ | parentage |
| 1 | 5.77 | C ₆₀ | 11 | 4.13 | C ₆₀ |
| 2 | 5.74 | C ₆₀ | 12 | 4.08 | C ₆₀ |
| 3 | 5.70 | C ₆₀ | 13 | 3.83 | C ₆₀ |
| 4 | 5.68 | porphyrin | 14 | 3.30 | carotene |
| 5 | 5.60 | C ₆₀ | 15 | 3.13 | porphyrin |
| 6 | 5.56 | carotene | 16 | 3.09 | porphyrin |
| 7 | 5.25 | porphyrin | 17 | 3.03 | C ₆₀ |
| 8 | 5.00 | porphyrin | 18 | 3.00 | C ₆₀ |
| 9 | 4.97 | carotene | 19 | 2.88 | C ₆₀ |
| 10 | 4.30 | carotene | 20 | 2.71 | C ₆₀ |

occupied and lowest unoccupied orbitals (HOMO and LUMO) are found on the carotenoid and the C₆₀, respectively. The gap between these two levels with zero spatial overlap is 0.17 eV from eigenvalue difference. The details of the ground-state electronic structure can be found in ref 5.

Excited States

While the calculation of the ground state is straightforward, obtaining an accurate description of the excited states from DFT especially for the charge-separated particle-hole states is difficult. To understand the transitions between various components we first need to calculate the energies of the relevant excited states. For that purpose, we consider a set of the highest ten occupied orbitals and ten lowest unoccupied orbitals over an energy range of 3 eV. These sets of orbitals in consideration are listed in Table 4.

As listed in the table these orbitals are mostly on one component of the triad. We label the states by HN/PM where H(P) refers to the location of the hole (particle) which can be carotenoid (C), porphyrin, and buckyball (B). N,M refer to the state number given in Table 4. From these two sets of occupied and unoccupied orbitals we have derived a set of 100 singly excited particle-hole states. A number of these excited states have large overlap between the particle and the hole orbitals when both the orbitals are on the same component. We have carried out the method described above to estimate the excited-state energies. This computationally inexpensive approach incorporates the charge polarization effects and the long-range $1/R$ interaction between the particle and hole, referred to as “electron-transfer self-interaction”,³⁸ without requiring the added expense of a complete self-interaction correction^{9–11} treatment of the passive orbitals. In the separated fragment limit, the method correctly reproduces the CT excitation ($I - A - 1/R$) which depends only on ground-state quantities. For the porphyrin-porphyrin excitations, our corrected excitation energy (2.05 eV) differs only slightly from the eigenvalue difference (1.87 eV) and is in excellent agreement with experiment (1.98)³⁹ and TDLDA calculations (2.16 eV).⁴⁰ However, for the large dipole excitation where TDLDA has been shown to fail,³⁸ the eigenvalue difference of 0.17 eV dramatically underestimates our corrected excitation energy of 2.46 eV in good agreement with an estimate based on the carotenoid ionization energy, the fullerene affinity, and the fullerene-carotenoid

separation ($I - A - 1/R = 2.5$ eV). Our TDDFT calculation on the excitation of the triad also does not yield the charge-transfer energies.⁴¹

Polarization

The dipole moments of some of the singly excited particle-hole states are quite large (~ 171 Debye). The electric field of such large dipoles will in turn induce dipoles on the nearby molecules or on the solvents around them. The electric field due to these induced dipoles in turn stabilizes the dipole state. The solvent polarization is important since the photoinduced charge separation is observed when experiments have been performed on molecules solvated in 2-methyltetrahydrofuran or benzonitrile but not in toluene. Similar dipole-induced polarization will also appear in a molecular crystal as well. We demonstrate below that in the molecular crystal the dipole induced polarization will lower the energies of the excited states, and this stabilization depends on the square of the dipole moments and also on the molecular volume or concentration. This is demonstrated by considering the energy of a classical array of polarizable particles on a lattice. To estimate the orientation and lattice packing of an assembly of the triad, we have optimized the total energy of a dimer assuming a classical van-der-Waals (vdW) pair potential between the atoms on different molecules. The intramolecular bonds are held rigid during this procedure. The triad dimerizes such that the total dipole moment vanishes. Further DFT calculations on the dimer suggest that the repulsive interaction is significantly underestimated by the available vdW parameters, and the dimer cell volume thus derived is likely to be a lower bound. However, the stabilization energy can still be estimated in terms of the dimers at lattice positions. The stabilization energy is $\Delta E_i = E_x^i - E_g$, where E_x^i is the energy of the lattice with the central molecule in the i^{th} excited-state and E_g is the energy of the lattice with the ground-state dimer at each site. The energy of the dipole lattice is calculated variationally using a method developed for determining the dielectric constant of a fullerene crystal from the molecular polarizability and unit cell volumes (see ref 42). This energy is written as

$$E = \frac{1}{2} \sum_{\mu \neq \nu} \left[\frac{\vec{p}_\mu \cdot \vec{p}_\nu}{|\vec{r}_{\mu\nu}|^3} - \frac{3(\vec{p}_\mu \cdot \vec{r}_{\mu\nu})(\vec{p}_\nu \cdot \vec{r}_{\mu\nu})}{|\vec{r}_{\mu\nu}|^5} \right] + \sum_{\mu, \nu} \frac{1}{2} \vec{p}_\mu^i \alpha_{\mu\nu}^{-1} \vec{p}_\nu^i \delta_{\mu\nu} \quad (9)$$

In the above equation \vec{p}_μ and \vec{p}_ν are the total and induced dipole at lattice position \vec{r}_μ and $\vec{r}_{\mu\nu} = \vec{r}_\mu - \vec{r}_\nu$. The polarizability tensor α is calculated from self-consistent total energy and dipole moment of the molecule as a function of various applied electric field along the three Cartesian directions.^{42–44} The eigenvalues of the polarizability tensor are 878, 220, and 199 Å³ where the first eigenvector is along the molecular axis. The stabilization energy also depends on the molecular volume and orientation. The stabilization energies of a few excited states with large dipole moments are shown in Figure 2. The stabilization of the large dipole states depend critically on the molecular volume as can be

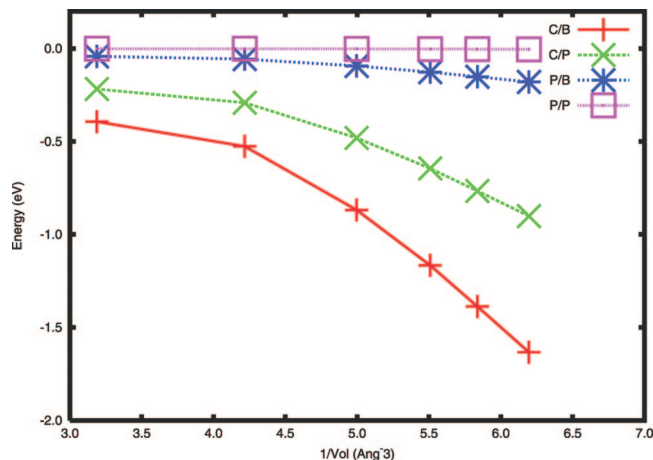


Figure 2. Change in energy levels of four excited states due to polarization effects. The labels C, P, and B refer to carotenoid, porphyrin, and buckyball. A/B refers to hole and particle localizations. The stabilization energy as a function of molecular volume is shown for lattice model.

seen from the figure. We find that it is necessary to increase the vdW dimer volume to avoid polarization induced divergences for the large dipole states (C10/B11–13 in our notation).

The polarization induced divergence is also present in the Clausius-Mossotti expression which relates the dielectric constant to the ratio of the polarizability to unit-cell volume. This divergence is not entirely unphysical as it is to some degree reflecting the fact that a crystal composed of highly polarizable particles will indeed breakdown when either a large enough internal or external electric field is applied. In a real system, this dielectric breakdown could be avoided by moving the charges.

The polarization lowers the energies of the large dipole states significantly bringing the theoretical energy levels closer to the experimental ones. In Figure 2 the stabilization of some of the particle-hole states are plotted as a function of inverse volume. Due to their small dipole moments, the ground and the porphyrin-porphyrin excited-state energies are nearly unaffected by cell volumes. Reduction of the transverse cell dimensions lowers the large-dipole excited states energies steeply leading to polarization induced breakdown. The stabilization energy decreases monotonically with increasing volume.

Dipole Transition Probabilities for KMC

In the experiment the triggering radiation was sent as a pulsed laser at 590 nm which corresponds to the porphyrin absorption frequency.¹ It was observed by Liddel et al. that the final charge separated state was reached following a series of transitions involving the P*-C₆₀⁺, P*-C₆₀⁻, and the C+-P-C₆₀⁻ states.

When bathed in a radiation density similar to that of sunlight, a large number of dipole allowed transitions between various electronic states as well as vibronic states can occur. In this paper, we concentrate only on the electronic dipole-allowed transitions and examine whether a sequence of dipole allowed transition can lead to one of the charge-

separated states. To find the possible sequence of radiative transitions leading to the charge-separated state, we have calculated Einstein's A and B coefficients. At this stage, the transition probabilities are calculated at temperature $T = 0$ and only to first-order. These probabilities are then used in a kinetic Monte-Carlo simulation to obtain the risetime of the charge-separated states.

The transition probability γ is determined as $\gamma_{ij} = A_{ij}\Theta(\epsilon_i - \epsilon_j) + B_{ij}u(\omega_{ij})$ and $\gamma_{ii} = -\sum_j \gamma_{ij}$. Note that the spectral power distribution contains an Arrhenius-like factor of $e^{-\Delta/kT}$ with Δ being the relevant excitation energy. B_{ij} is obtained from the dipolar transition matrix elements between the particle-hole states constructed from the unperturbed ground-state Kohn–Sham orbitals and $A_{ij} = (2\hbar\omega^3/\pi^2c^3)B_{ij}$.⁴⁶ The incident solar radiation with energy density $u(\omega)d\omega$ can be simulated as blackbody radiation at temperature $T = 6000$ K attenuated by a factor (R_s^2/D^2) where R_s and D are the radii of the sun and average earth trajectory. The lifetime of the i^{th} state is $\tau = \gamma_{ii}^{-1}$. At each $\tau/20$, the transition is determined to happen if a random number is less than 1/20. At this point a second random number is used to determine to which state the molecule evolves. This is weighted to ensure correct branching ratios stipulated by $1/\gamma_{ij}$. First, the simulations were carried out for a million steps, and the total time spent in each state is noted. The Einstein A and B coefficients depend on dipole matrix elements between particle and hole states.

In this work we have used the ground-state Kohn–Sham orbitals for estimating the dipole matrix elements. However, a more accurate and more involved approach to calculating these dipole matrix elements would be to calculate the many-electron dipole matrix element between the two Slater determinants. This would account for both direct and indirect relaxation effects. By direct, we refer to the fact that the particle state relaxes slightly due to the change in density. For the dipole matrix elements that connect the HOMO and LUMO porphyrin levels we find that this effect is quite small and that the matrix elements change by less than 1.5%. We also point out that there are other small corrections to this approximation at the many-electron level since the passive orbitals have also been allowed to relax. Inclusion of such effects would certainly be an improvement.

The Monte-Carlo simulations are first carried out for the molecule in gas phase. The large dipole states C10/B11–13 lie above the ground state by 2.46, 2.51, and 2.80 eV. The porphyrin excited state lies about 2 eV above the ground state. The dipole moments of these states are nearly 171 Debye. In the isolated molecule, the incident solar radiation fails to excite the molecule to any of the large dipole states. This situation is similar to when the experiments are done using toluene as solvent. Experimentally, CT is not observed when the triad is solvated in toluene (dipole moment $\mu = 0.375$ D) but is observed in 2-MTHF ($\mu = 1.47$ D) and benzonitrile ($\mu = 4.18$ D).¹ Carbonera et al. have estimated from electrochemical measurements that the energy of the charge separated state in 2-MTHF is 1.24 eV above the ground state.⁴⁵ This is clearly an effect of the solvent polarization. The polar solvent encourages CT by lowering the energy of the CT states. If the polarization is ignored,

Table 5. Mean Time and Number of Transitions to Reach the Carotenoid/Buckyball States versus Applied Bias

| E_d (a.u.) | time (s) | transitions |
|--------------|----------------------|-------------------|
| 0.0000 | inf | |
| -0.0010 | 5.2 | 1.3×10^5 |
| -0.0020 | 0.06 | 1448.7 |
| -0.0030 | 5.5×10^{-3} | 175.1 |
| -0.0040 | 4.3×10^{-4} | 68.2 |
| -0.0050 | 7.4×10^{-5} | 70.1 |

then the large dipole states C10/B11–13 lie above the porphyrin excited states. Also the energy ordering of these states does not match that of the experiment without accounting for polarization of the solvents. The molecule spends 99.8% of its time in the ground state. As we have mentioned earlier the energy shift due to polarization depends on the molecular volume. We have estimated the time taken to reach any of the charge-transfer states from carotenoid HOMO to any one of the C_{60} T_{1u} LUMO states taking into account the energy shifts due to polarization. These are the lowest energy states with a hole in the carotenoid and a particle on the buckyball. For these calculations, a molecular volume of $100 \times 35 \times 35$ {a.u.}³ was chosen. This volume reduces the energies of the lowest HOMO–LUMO transition to 1.17 eV, close to the experimental values. The Monte-Carlo simulations were allowed to go up to 10 million steps in a given run, and the runs were repeated for 100,000 times to obtain good averages. We find that on average about 62 s are taken to reach the target CT states. This is slower compared to charge transfer in biological systems and not fast enough for a useful solar cell.

Another situation where the energies of the CT states will be lowered is when there are counterions present in the surrounding. One way of testing this hypothesis is to apply a bias field to lower the energies of the dipole states. Applied negative bias along the direction of the largest dipole moment state will lower the energy of that state. We have carried out this test by applying a uniform field in the range of -0.005 au to +0.005 au along the dipoles of the excited states of interest. The average time taken to reach any of the carotenoid-buckyball CT states is shown in Table 5. The initial state in this calculation was taken as the ground state. The average risetime is calculated from 10^5 such samplings. We note that in the actual sample the field will not be a uniform one. The local electric field in the sample can be caused by a large dipole moment of a neighboring excited molecule (possibly) or due to the presence of counterions and/or polar solvents in the environment (definitely). A similar counterion activated charge transfer is shown to occur in a DNA molecule in ref 47. A field of the order of 0.001 au can be easily created by counterions. To illustrate the possibility of large counterion induced electric fields we have placed a dissociated Na^+Cl^- pair about 7 Å from C_{60} and the carotenoid center. This leads to an average electric field on the order of 0.0013 au. SCF calculations demonstrate the emergence of a large dipole. This effect is nearly independent of counterion type.

Carbonera et al. have proposed a CT reaction pathway which includes the porphyrin excited-state and also buckyball singlet to triplet excitations leading finally to the $C^+P-C_{60}^-$

state.⁴⁵ We have ignored the spin polarization and spin–orbit interaction to limit the computational expenses. Our calculations show that in the absence of solvent polarization, the $C^+P-C_{60}^-$ state lies about 0.3–0.4 eV above the porphyrin excited states. Thus incident radiation is necessary to excite the triad to the large dipole state. The difference in the energies arises because the experiments are carried out on molecules solvated in a polar media. The polarization effects would also occur in a lattice of molecules although it is different from the solvent effect. These polarization effects can change excited-state ordering and will be treated self-consistently in future. In the future, we will also include the nonradiative vibration assisted transitions in our calculations.

In summary, we present and discuss a method to calculate the excited-state energies from density-functional theory and apply it to calculate the energies of the charge-transfer states. We have carried out a DFT-based calculation on the radiative transitions on a large molecular triad. We present a scheme to calculate the charge-transfer energies from DFT which is computationally efficient. The method has been applied it to a large molecular triad. The charge separated states have large dipole moments. We show that medium polarization would lower the energies of the charge-separated states with large dipole moments. We examine the charge-transfer process using a kinetic Monte Carlo approach where we use Einstein's A and B coefficients. We show that the transition to the charge-separated states is catalyzed by several factors such as applied electric field and most notably the presence of counterions in the material. The one-second charging time obtained here suggests an absorption power of ~ 30 – 100 mWatt/m² per monolayer of the molecule. In the presence of counterions in the solvent, the transition to a charge separated state can trigger a domino-like effect.

Acknowledgment. The authors acknowledge ONR (Grant No. N000140211046) and the DoD CHSSI Program. T.B. acknowledges a UTEP startup grant, URI, NSF Advance program at UTEP, and NSF Grants No. HRD-0317607 and NIRT-0304122. T.B. gratefully acknowledges the Texas Advanced Computing Center (TACC) at The University of Texas at Austin for providing HPC resources that have contributed to part of the research results reported within this paper. Part of the calculations were performed on Cray XD1 at UTEP. Other parts of the work were performed on the SGI-Altix system at NRL-DC under the auspices of the DoD HPCMP. The authors thank CCS, NRL, especially W. L. Anderson and Dr. Jeanie E. Osburn, for providing computational resources. We thank John Perdew for sharing his wisdom and functionals on many occasions.

References

- (1) Liddell, P. A.; Kuciauskas, D.; Sumida, J. P.; Nash, B.; Nguyen, D.; Moore, A. L.; Moore, T. A.; Gust, D. *J. Am. Chem. Soc.* **1997**, *119*, 1400.
- (2) Smirnov, S. N.; Liddell, P. A.; Vlassioul, I. V.; Teslja, A.; Kuciauskas, D.; Braun, C. L.; Moore, A. L.; Moore, T. A.; Gust, D. *J. Phys. Chem. A* **2003**, *107*, 7567.
- (3) Kuciauskas, D.; Liddell, P. A.; Lin, S.; Stone, S. G.; Moore, A. L.; Moore, T. A.; Gust, D. *J. Phys. Chem. B* **2000**, *104*, 4307.

- (4) Andreasson, J.; Kodis, G.; Terazono, Y.; Liddell, P. A.; Bandyopadhyay, S.; Mitchell, R. H.; Moore, T. A.; Moore, A. L.; Gust, D. *J. Am. Chem. Soc.* **2004**, *126*, 15926.
- (5) Baruah, T.; Pederson, M. R. *J. Chem. Phys.* **2006**, *125*, 164706.
- (6) Davidson, E. R.; Nitzsche, L. E. *J. Am. Chem. Soc.* **1979**, *101*, 6524.
- (7) Levy, M.; Perdew, J. P. *Phys. Rev. B* **1985**, *31*, 6264.
- (8) Callaway J.; March N. H. *Solid State Physics*; Academic: New York, 1984.
- (9) Perdew, J. P.; Zunger, A. *Phys. Rev. B* **1981**, *23*, 5048.
- (10) Pederson, M. R.; Heaton, R. A.; Lin, C. C. *J. Chem. Phys.* **1985**, *82*, 2688.
- (11) Heaton, R. A.; Pederson, M. R.; Lin, C. C. *J. Chem. Phys.* **1987**, *86*, 258.
- (12) Perdew, J. P.; Burke, K.; Ernzerhof, M. *Phys. Rev. Lett.* **1996**, *77*, 3865.
- (13) Porezag, D. V.; Pederson, M. R. *Phys. Rev. A* **1999**, *60*, 2840.
- (14) Pederson, M. R.; Porezag, D. V.; Kortus, J.; Patton, D. C. *Phys. Status Solidi B* **2000**, *217*, 197.
- (15) Pederson, M. R.; Jackson, K. A. *Phys. Rev. B* **1990**, *41*, 7453.
- (16) Pederson, M. R.; Jackson, K. A. *Phys. Rev. B* **1991**, *43*, 7312.
- (17) Jackson, K. A.; Pederson, M. R. *Phys. Rev. B* **1990**, *42*, 3276.
- (18) Andersson, C. K. T.; Sundstrom, J.; Kiyan, I. Y.; Hanstorp, D.; Pegg, D. J. *Phys. Rev. A* **2000**, *62* (111), 022503.
- (19) Ruzsinszky, A.; Perdew, J. P.; Csonka, G. I.; et al. *J. Chem. Phys.* **2007**, *126*, 104102.
- (20) Ruzsinszky, A.; Perdew, J. P.; Csonka, G. I.; et al. *J. Chem. Phys.* **2006**, *125*, 194112.
- (21) Ossowski, M. M.; Boyer, L. L.; Mehl, M. J.; Pederson, M. R. *Phys. Rev. B* **2003**, *68*, 245107.
- (22) Tozer, D. J.; De Proft, F. *J. Phys. Chem. A* **2005**, *109*, 8923.
- (23) Compton, R. N.; Tuinman, A. A.; Klots, C. E.; Pederson, M. R.; Patton, D. C. *Phys. Rev. Lett.* **1997**, *78*, 4367.
- (24) Hettich, R. L.; Compton, R. N.; Ritchie, R. H. *Phys. Rev. Lett.* **1991**, *67*, 1242.
- (25) Watson, R. E. *Phys. Rev.* **1958**, *111*, 1108.
- (26) Boyer, L. L. *Phys. Rev. Lett.* **1985**, *54*, 1940.
- (27) Wu, Q.; Van Voorhis, T. *J. Chem. Phys.* **2006**, *125*, 164105.
- (28) Wu, Q.; Van Voorhis, T. *J. Chem. Theory Comput.* **2006**, *2*, 765–774.
- (29) Wu, Q.; Cheng, C. L.; Van Voorhis, T. *J. Chem. Phys.* **2007**, *127*, 164119.
- (30) Theophilou, A. K. *J. Phys. C* **1979**, *12*, 5419.
- (31) Lowdin, P. O. *J. Chem. Phys.* **1950**, *18*, 365.
- (32) Marshal, D. Ph.D. Thesis, University of Wisconsin, 2006.
- (33) Tilford, S. G.; Simmons, J. D. *J. Phys. Chem. Ref. Data* **1972**, *1*, 147.
- (34) Krupenie, P. H. *J. Phys. Chem. Ref. Data* **1972**, *1*, 423.
- (35) Lofthus, A.; Krupenie, P. H. *J. Phys. Chem. Ref. Data* **1972**, *6*, 113.
- (36) Swanson, N.; Celotta, R. J. *Phys. Rev. Lett.*, **1975**, *35*, 783.
- (37) Boutalib, A.; Gadea, F. X. *J. Chem. Phys.* **1992**, *97*, 1144.
- (38) Dreuw, A.; Head-Gordon, M. *J. Am. Chem. Soc.* **2004**, *126*, 4007.
- (39) Edwards, L.; Dolphin, D. H.; Gouterman, M.; Adler, A. D. *J. Mol. Spectrosc.* **1971**, *38*, 16.
- (40) Gisbergen, S. J. A.; Rosa, A.; Ricciardi, G.; Baerends, E. J. *J. Chem. Phys.* **1999**, *111*, 2499.
- (41) Spallanzani, N.; Rozzi, C. A.; Varsano, D.; Manghi, F.; Rubio, A.; Baruah, T.; Pederson, M. R. To be published.
- (42) Pederson, M. R.; Quong, A. A. *Phys. Rev. B* **1992**, *46*, 13584.
- (43) Zope, R. R.; Baruah, T.; Pederson, M. R.; Dunlap, B. *Int. J. Quantum Chem.* **2008**, *108*, 307.
- (44) Pederson, M. R.; Baruah, T. *Lect. Ser. Comput. Comput. Chem.* **2005**, *3*, 156.
- (45) Carbonera, D.; Valentin, M. D.; Corvaja, C.; Agostini, G.; Giacometti, G.; Liddell, P. A.; Kuciauskas, D.; Moore, A. L.; Moore, T. A.; Gust, D. *J. Am. Chem. Soc.* **1998**, *120*, 4398.
- (46) Slater, J. C. *Quantum Theory of Matter*; McGraw Hill Book Company: 1951.
- (47) Barnett, R. N.; Cleveland, C. L.; Joy, A.; Landman, U.; Schuster, G. B. *Nature* **2001**, *294*, 567.